Available online at www.sciencedirect.com

ScienceDirect

IFAC Papers Online CONFERENCE PAPER ARCHIVE

IFAC PapersOnLine 55-31 (2022) 13–18

Adaptive Non-Singular Terminal Sliding Mode Tracking Control of an UUV Against Disturbances

V. Sebastian Martinez-Perez * **Andres E. Sanchez-Calvo** *
Alejandro Gonzalez-Garcia * **Herman Castañeda** *

* *Tecnologico de Monterrey, School of Science and Engineering, Monterrey, N.L., Mexico. (e-mail: a01232474@tec.mx, a01351370@tec.mx, alexglzg97@gmail.com, hermancc@tec.mx).*

Abstract: A robust design of a trajectory tracker for an unmanned underwater vehicle under the influence of disturbances is addressed in this article. The controller policy is formulated upon an adaptive sliding mode approach, where a manifold of a non-singular terminal sliding mode ensures the tracking errors to converge to a locality close to zero in practical finite-time. Moreover, the adaptation dynamics allow no overestimation of control gains, reducing chattering as well as the control efforts, and maintain robustness against external perturbations with unknown boundaries. Simulation results conducted in a full mathematical model of the craft showcase the performance and feasibility of the suggested method to track the desired references, even with the vehicle subject to water currents.

Keywords: Unmanned underwater vehicle, UUV robust control, non-singular terminal sliding mode control, adaptive sliding mode.

1. INTRODUCTION

For the past two decades, researchers and industries have increased their interest in studying and exploring the underwater environment, as explained in Zereik et al. (2018), raising the demand for Unmanned Underwater Vehicles (UUVs) to reduce the costs and dangers of exposing a man to a deep-sea and high-pressure work environment. These vehicles have become substantial for applications such as ship maintenance, seabed mapping, species monitoring, gas and oil inspection, offshore exploration of minerals, maintenance of sub-aquatic infrastructure, and pipeline surveys, to name a few (Karimi and Lu, 2021; Yu et al., 2019; Christ and Wernli, 2014).

Vehicle operation for these tasks usually require high performance control laws for path-following or trajectory tracking objectives. The former objective examines the design of a controller for driving the craft states to follow a time-independent path, different from the latter objective, which considers temporal constraints. Furthermore, UUVs must deal with environmental disturbances such as water currents and system uncertainties present in the form of nonlinear coupled and unmodeled dynamics (Fossen, 2011). Moreover, as the mass of mini UUVs, as stated in Christ and Wernli (2014), does not exceed 32 kg, the effect of such disturbances is greater in comparison to heavier common crafts, so perturbation rejection must be considered for the control design of these vehicles.

Motivated by the mentioned challenges, trajectory tracking control for UUVs is currently an active research topic. For instance, in Jia et al. (2020), a tracker is proposed using a passivity-based method and Port Hamiltonian theory that is able to address external perturbations and model uncertainties, nonetheless, tracking errors converge asymptotically and only constant disturbances are considered. In Suarez et al. (2018), a control strategy derived from a second order filter and a PD controller for disturbance rejection is addressed for depth trajectories, although results are limited, as only motion in heave is analyzed. In Hasan and Abbas (2022), an adaptive fuzzy within a nonlinear PID control is suggested to reject disturbances and model uncertainties, however, the tracking errors converge asymptotically. In Gong et al. (2021) a Lyapunov-based backstepping technique combined with a double-looped MPC that deals with water currents was investigated. Nevertheless, the above references exhibited limited robustness.

An outstanding technique that addresses the aforementioned problems is the Sliding Mode Control (SMC), which provides insensitivity to parameter variations and robustness to unmodeled dynamics and external disturbances (Utkin, 1993). The principal inconvenient of the conventional SMC is the existence of chattering, a high-frequency oscillation phenomena in the control signals, undesirable in practical applications as it wears out vehicle actuators (Utkin and Lee, 2006). Adaptive SMC (ASMC) (Utkin and Poznyak, 2013) is a method that mitigates chattering by computing varying gains that avoid overestimation of control efforts, and also provide the advantage of not requiring knowledge on the bounds of disturbances and uncertainties. An adaptive dynamical SMC methodology for tracking control for underactuated underwater vehicles is suggested to deal with external disturbances and model uncertainties (Xu et al., 2015). In Rodriguez et al. (2020), an ASMC is designed for a micro AUV under uncertainties

10.1016/j.ifacol.2022.10.402

and water currents. Higher-Order SMC (HOSMC) and Super-Twisting SMC (STSMC) can also attenuate chattering (Shtessel et al., 2014). Manzanilla et al. (2021) studied a Super-Twisting Integral SMC (STISMC) for chattering attenuation and bounded disturbance compensation.

A drawback of SMCs, and of previous methods by extension, is that tracking errors converge asymptotically even when the sliding surface converges in finite-time, which in practical applications might not be an issue, but if a high steady-state precision is required, large control efforts would be demanded (Yu et al., 2020). Terminal SMC (TSMC) was introduced to guarantee tracking error convergence in finite-time (Venkataraman and Gulati, 1992), with the inconvenience of a singularity in the control design (Wu et al., 1998), which was later solved by the proposal of the Non-Singular TSMC (NTSMC) (Feng et al., 2002; Yu et al., 2005). In Londhe et al. (2017), a NTSMC was designed for controlling an underactuated UUV, however, the scheme presented the problem of requiring to know in advance the bounds of the disturbances. Variations of NTSMC for UUVs exist, such as Rangel et al. (2020), where an Adaptive NTSMC (ANTSMC) is designed; the approach ensures finite-time tracking error convergence to a bounded region, even subject to model uncertainties and disturbances. An Adaptive Non-Singular Integral TSMC (ANITSMC) is addressed in Qiao and Zhang (2017) to guarantee finite-time local convergence for velocity tracking errors, followed by an exponential convergence for position tracking errors, even under the influence of model uncertainties and perturbations. An Adaptive Fast NITSMC (AFNITSMC) was proposed to further improve the previous method (Qiao and Zhang, 2020).

In this article, a proposal of a robust controller for a fully-actuated mini UUV subject to water currents is described. The control law is addressed as an Adaptive Non-Singular Terminal Sliding Mode Control (ANTSMC), capable of driving tracking errors to converge in practical finite-time to a set close to zero. The adaptive gains reduce the chattering effect, as the control gains are not overestimated, and provide robustness to bounded disturbances and uncertainties, whose upper bounds are unknown. To confirm the advantages and feasibility of the suggested scheme, simulations are conducted in a full 6-DOF mathematical model of the UUV subject to water currents.

The content of this article is ordered as shown. The dynamic and kinematic model of the UUV is explained, alongside the model of water currents, in Section 2. The ANTSMC design is detailed in Section 3. The results and discussion on the controller performance are addressed in Section 4. At last, conclusions are presented.

2. MATHEMATICAL MODELING

The UUV dynamic and kinematic model is described in the current section, as well as a description of the external disturbances acting on the vehicle.

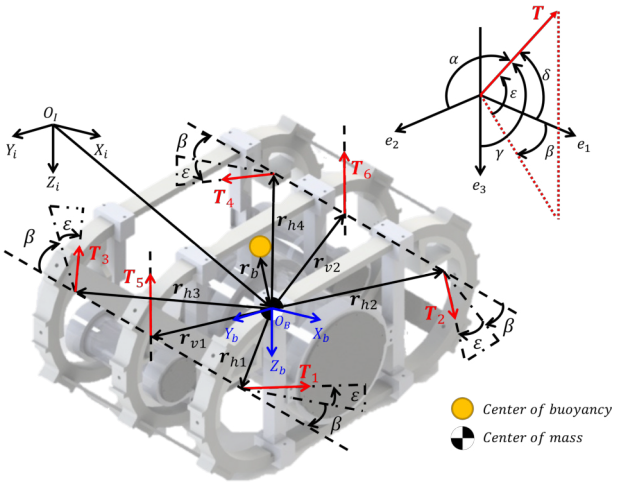

Fig. 1. Inertial frame O_I, body-fixed frame O_B and thruster frame (upper-right corner)

2.1 UUV dynamic and kinematic model

To describe the dynamic and kinematic model of the UUV, the inertial and the body-fixed frames are required (Fig. 1). Following the robot-like vectorial model presented in Fossen (2011), the 6-DOF UUV motion equations are described as:

$$\dot{\boldsymbol{\eta}} = \boldsymbol{J}(\boldsymbol{\eta})\boldsymbol{\nu} \tag{1}$$

$$\boldsymbol{M}\dot{\boldsymbol{\nu}} + \boldsymbol{C}(\boldsymbol{\nu})\boldsymbol{\nu} + \boldsymbol{D}(\boldsymbol{\nu})\boldsymbol{\nu} + \boldsymbol{g}(\boldsymbol{\eta}) = \boldsymbol{\tau} \tag{2}$$

Equation (1) describes the vehicle kinematics, where the position and attitude vector $\boldsymbol{\eta} = [x, y, z, \phi, \theta, \psi]^T$ is defined in the inertial frame, the vector $\boldsymbol{\nu} = [u, v, w, p, q, r]^T$ of linear and angular velocities is expressed in the body referential frame, and the matrix $\boldsymbol{J}(\boldsymbol{\eta})$ is described by:

$$\boldsymbol{J}(\boldsymbol{\eta}) = \begin{bmatrix} \boldsymbol{R}(\boldsymbol{\eta}) & \boldsymbol{0}_{3x3} \\ \boldsymbol{0}_{3x3} & \boldsymbol{T}(\boldsymbol{\eta}) \end{bmatrix} \tag{3}$$

$$\boldsymbol{R}(\boldsymbol{\eta}) = \begin{bmatrix} \mathrm{c}\psi\mathrm{c}\theta & -\mathrm{s}\psi\mathrm{c}\phi + \mathrm{c}\psi\mathrm{s}\theta\mathrm{s}\phi & \mathrm{s}\psi\mathrm{s}\phi + \mathrm{c}\psi\mathrm{c}\phi\mathrm{s}\theta \\ \mathrm{s}\psi\mathrm{c}\theta & \mathrm{c}\psi\mathrm{c}\phi + \mathrm{s}\phi\mathrm{s}\theta\mathrm{s}\psi & -\mathrm{c}\psi\mathrm{s}\phi + \mathrm{s}\theta\mathrm{s}\psi\mathrm{c}\phi \\ -\mathrm{s}\theta & \mathrm{c}\theta\mathrm{s}\phi & \mathrm{c}\theta\mathrm{c}\phi \end{bmatrix} \tag{4}$$

$$\boldsymbol{T}(\boldsymbol{\eta}) = \begin{bmatrix} 1 & \mathrm{s}\phi\mathrm{t}\theta & \mathrm{c}\phi\mathrm{t}\theta \\ 0 & \mathrm{c}\phi & -\mathrm{s}\phi \\ 0 & \mathrm{s}\phi/\mathrm{c}\theta & \mathrm{c}\phi/\mathrm{c}\theta \end{bmatrix} \tag{5}$$

with c(·), s(·) and t(·) representing cos(·), sin(·) and tan(·) respectively.

Equation (2) describes the dynamics of the vehicle, with $\boldsymbol{M}$ being the inertia matrix, considering added mass and rigid-body terms:

$$\boldsymbol{M} = \mathrm{diag}(m - X_{\dot{u}}, m - Y_{\dot{v}}, m - Z_{\dot{w}}, I_{xx} - K_{\dot{p}}, I_{yy} - M_{\dot{q}}, I_{zz} - N_{\dot{r}}) \tag{6}$$

The addition of the coriolis added mass and rigid-body matrices defines the matrix $\boldsymbol{C}(\boldsymbol{\nu})$:

$$\boldsymbol{C}(\boldsymbol{\nu}) = \begin{bmatrix} 0 & 0 & 0 & 0 & a_3 & -a_2 \\ 0 & 0 & 0 & -a_3 & 0 & a_1 \\ 0 & 0 & 0 & a_2 & -a_1 & 0 \\ 0 & a_3 & -a_2 & 0 & -b_3 & b_2 \\ -a_3 & 0 & a_1 & b_3 & 0 & -b_1 \\ a_2 & -a_1 & 0 & -b_2 & b_1 & 0 \end{bmatrix} \tag{7}$$

where $a_1 = mu - X_{\dot{u}}u$, $a_2 = mv - Y_{\dot{v}}v$, $a_3 = m\omega - Z_{\dot{\omega}}\omega$, $b_1 = I_{xx}p + K_{\dot{p}}p$, $b_2 = I_{yy}q + M_{\dot{q}}q$, and $b_3 = I_{zz}r + N_{\dot{r}}r$.

Table 1. VTec U-IV prototype parameters

Parameter	Value	Parameter	Value
Length	0.48 [m]	I_{yy}	1.75 [kg m^2]
Height	0.36 [m]	I_{zz}	1.43 [kg m^2]
Beam	0.72 [m]	$X_{\dot{u}}$	16.8374 [kg]
m	24 [kg]	$Y_{\dot{v}}$	20.2748 [kg]
Volume	0.0252 [m^3]	$Z_{\dot{w}}$	35.318 [kg]
W	235.44 [N]	$K_{\dot{p}}$	0.2165 [kg]
B	245 [N]	$M_{\dot{q}}$	0.6869 [kg]
β	15 [deg]	$N_{\dot{r}}$	0.6157 [kg]
ε	20 [deg]	X_u	-0.3431 [N m^{2}s^{-1}]
α	75.92 [deg]	Y_v	0.0518 [N m^{2}s^{-1}]
δ	24.81 [deg]	Z_w	-0.5841 [N m^{2}s^{-1}]
γ	105 [deg]	K_p	0.0064 [N m^{2}s^{-1}]
$r_{b,z}$	-0.10726 [m]	M_q	0.04 [N m^{2}s^{-1}]
r_{hx}	0.1867 [m]	N_r	-0.1063 [N m^{2}s^{-1}]
r_{hy}	0.2347 [m]	$X_{\|u\|u}$	-111.7397 [N m^{2}s^{-2}]
r_{hz}	0.0175 [m]	$Y_{\|v\|v}$	-44.4058 [N m^{2}s^{-2}]
r_{vx}	0 [m]	$Z_{\|\omega\|\omega}$	-157.1951 [N m^{2}s^{-2}]
r_{vy}	0.2384 [m]	$K_{\|p\|p}$	-0.4634 [N m^{2}s^{-2}]
r_{vz}	0 [m]	$M_{\|q\|q}$	-0.2902 [N m^{2}s^{-2}]
I_{xx}	0.9 [kg m^2]	$N_{\|r\|r}$	-2.2897 [N m^{2}s^{-2}]

The matrix $\boldsymbol{D}(\boldsymbol{\nu})$ is composed by the addition of damping nonlinear and linear matrices:

$$\boldsymbol{D}(\boldsymbol{\nu}) = -\text{diag}(X_u + X_{|u|u}|u|, Y_v + Y_{|v|v}|v|, Z_\omega + Z_{|\omega|\omega}|\omega|, K_p + K_{|p|p}|p|, M_q + M_{|q|q}|q|, N_r + N_{|r|r}|r|) \quad (8)$$

Furthermore, the restorative forces and torques vector $\boldsymbol{g}(\boldsymbol{\eta})$ generated by the buoyancy and weight forces is addressed as:

$$\boldsymbol{g}(\boldsymbol{\eta}) = \begin{bmatrix} (W-B)\text{s}\theta \\ -(W-B)\text{c}\theta\text{s}\phi \\ -(W-B)\text{c}\theta\text{c}\phi \\ -r_{b,z}B\text{c}\theta\text{s}\phi \\ -r_{b,z}B\text{s}\theta \\ 0 \end{bmatrix} \quad (9)$$

where $r_{b,z}$ is the vertical distance from the center of mass to the center of buoyancy. Finally, the input forces vector $\boldsymbol{\tau}$ is defined as:

$$\boldsymbol{\tau} = \begin{bmatrix} (T_1 + T_2 - T_3 - T_4)|\text{c}\delta| \\ (-T_1 + T_2 - T_3 + T_4)|\text{c}\alpha| \\ -(T_5 + T_6) + (-T_1 - T_2 + T_3 + T_4)|\text{c}\gamma| \\ (-T_1 + T_2)\lambda_1 + (T_3 - T_4)\lambda_2 + (-T_5 + T_6)r_{vy} \\ (T_1 + T_2)\lambda_3 + (T_3 + T4)\lambda_4 \\ (-T_1 + T_2 + T_3 - T_4)\lambda_5 \end{bmatrix} \quad (10)$$

where $|T_i| < 35$ N, for $i = 1, 2, 3, 4, 5, 6$, are thruster magnitudes, $\lambda_1 = r_{hy}|\text{c}\gamma| + r_{hz}|\text{c}\alpha|$, $\lambda_2 = r_{hy}|\text{c}\gamma| - r_{hz}|\text{c}\alpha|$, $\lambda_3 = r_{hx}|\text{c}\gamma| - r_{hz}|\text{c}\delta|$, $\lambda_4 = r_{hx}|\text{c}\gamma| + r_{hz}|\text{c}\delta|$, and $\lambda_5 = r_{hx}|\text{c}\alpha| + r_{hy}|\text{c}\delta|$. The thruster configuration shown in Fig. 1 for the VTec U-IV is a custom design under development that provides fully-actuation with no excessive number of thrusters and prioritizing longitudinal motion, yet, enabling lateral movement in a lesser degree. Thruster vector positions in the body-fixed frame follow $||\boldsymbol{r}_{h1}|| = ||\boldsymbol{r}_{h2}|| = ||\boldsymbol{r}_{h3}|| = ||\boldsymbol{r}_{h4}|| = \sqrt{{r_{hx}}^2 + {r_{hy}}^2 + {r_{hz}}^2}$ and $||\boldsymbol{r}_{v1}|| = ||\boldsymbol{r}_{v2}|| = \sqrt{{r_{vx}}^2 + {r_{vy}}^2 + {r_{vz}}^2}$, and thrust vectors have direction β and tilt ε. Finally, the VTec U-IV model parameters can be found in Table 1, estimated employing strip theory and computational fluid dynamics methods (Eidsvik, 2015).

Differentiating (1) with respect to time yields (11), which is in turn used to express the dynamic model in the inertial frame, resulting in (12).

$$\dot{\boldsymbol{\nu}} = \boldsymbol{J}^{-1}(\ddot{\boldsymbol{\eta}} - \dot{\boldsymbol{J}}\boldsymbol{J}^{-1}\boldsymbol{\eta}) \quad (11)$$

$$\ddot{\boldsymbol{\eta}} = -\bar{\boldsymbol{M}}^{-1}(\bar{\boldsymbol{C}}(\boldsymbol{\eta}, \dot{\boldsymbol{\eta}})\dot{\boldsymbol{\eta}} + \bar{\boldsymbol{D}}(\boldsymbol{\eta}, \dot{\boldsymbol{\eta}})\dot{\boldsymbol{\eta}} + \boldsymbol{g}(\boldsymbol{\eta}) + \boldsymbol{\tau}) \quad (12)$$

where

$$\bar{\boldsymbol{M}} = \boldsymbol{M}\boldsymbol{J}(\boldsymbol{\eta})^{-1} \quad (13)$$

$$\bar{\boldsymbol{C}}(\boldsymbol{\eta}, \dot{\boldsymbol{\eta}}) = -\bar{\boldsymbol{M}}\dot{\boldsymbol{J}}\boldsymbol{J}^{-1} + \boldsymbol{C}(\boldsymbol{J}^{-1}\dot{\boldsymbol{\eta}})\boldsymbol{J}(\boldsymbol{\eta})^{-1} \quad (14)$$

$$\bar{\boldsymbol{D}}(\boldsymbol{\eta}, \dot{\boldsymbol{\eta}}) = \boldsymbol{D}(\boldsymbol{J}(\boldsymbol{\eta})^{-1}\dot{\boldsymbol{\eta}})\boldsymbol{J}(\boldsymbol{\eta})^{-1} \quad (15)$$

2.2 External disturbances model

For an UUV, external disturbances are found in the form of water currents. Similar to Fossen (2011), the model of current velocities follows a first order Gauss-Markov process described by:

$$\dot{U}_c + \mu U_c = \omega \quad (16)$$

$$V_c = U_c + \kappa \quad (17)$$

where V_c denotes the water current speed, ω a Gaussian noise, and $\mu \geq 0$ and κ are arbitrary constants. Then, the water current vector in the inertial frame is described by (18), where α_c and β_c specify the current direction.

$$\boldsymbol{\nu}_c = \begin{bmatrix} V_c\text{c}\alpha_c\text{c}\beta_c \\ V_c\text{s}\beta_c \\ V_c\text{s}\alpha_c\text{c}\beta_c \\ 0 \\ 0 \\ 0 \end{bmatrix} \quad (18)$$

Next, the dynamic model including water currents (Fossen, 2011) is expressed as:

$$\boldsymbol{M}\dot{\boldsymbol{\nu}} + \boldsymbol{C}_{RB}(\boldsymbol{\nu})\boldsymbol{\nu} + \boldsymbol{C}_A(\boldsymbol{\nu}_r)\boldsymbol{\nu}_r + \boldsymbol{D}(\boldsymbol{\nu}_r)\boldsymbol{\nu}_r + \boldsymbol{g}(\boldsymbol{\eta}) = \boldsymbol{\tau} \quad (19)$$

where $\boldsymbol{\nu}_r = \boldsymbol{\nu} - \boldsymbol{\nu}_c$. Finally, the model is rearranged as:

$$\boldsymbol{M}\dot{\boldsymbol{\nu}} + \boldsymbol{C}(\boldsymbol{\nu})\boldsymbol{\nu} + \boldsymbol{D}(\boldsymbol{\nu})\boldsymbol{\nu} + \boldsymbol{g}(\boldsymbol{\eta}) = \boldsymbol{\tau} + \boldsymbol{\gamma} \quad (20)$$

where $\boldsymbol{\gamma} = \boldsymbol{C}_A(\boldsymbol{\nu}_c)\boldsymbol{\nu}_c + \boldsymbol{D}(\boldsymbol{\nu}_c)\boldsymbol{\nu}_c$ are the external disturbances generated by the water current velocities.

3. TRACKING CONTROL DESIGN

The control strategy for achieving UUV trajectory tracking is addressed in the current section. The objective is for the UUV to track a time-varying desired trajectory, even under the influence of disturbances. In that sense, the controller is formulated on an adaptive non-singular terminal sliding mode approach.

3.1 ANTSMC design for UUVs

Consider a second order nonlinear dynamic system with external disturbances and model uncertainties as described below:

$$\begin{aligned} \dot{\boldsymbol{\chi}}_1 &= \boldsymbol{\chi}_2 \\ \dot{\boldsymbol{\chi}}_2 &= \boldsymbol{f}(\boldsymbol{\chi}_1, \boldsymbol{\chi}_2) + \boldsymbol{g}(\boldsymbol{\chi}_1, \boldsymbol{\chi}_2)\boldsymbol{u} + \boldsymbol{\Delta} \end{aligned} \quad (21)$$

where $\boldsymbol{\chi}_1 = \boldsymbol{\eta}$ and $\boldsymbol{\chi}_2 = \dot{\boldsymbol{\eta}}$ are the system states, $\boldsymbol{u} = \boldsymbol{\tau}$ is the control input, $\boldsymbol{\Delta}$ represent bounded model uncertainties and disturbances, and the nonlinear functions $\boldsymbol{f}(\cdot)$ and $\boldsymbol{g}(\cdot)$ are derived from dynamics (12):

$$\boldsymbol{f}(\boldsymbol{\chi}_1, \boldsymbol{\chi}_2) = -\bar{\boldsymbol{M}}^{-1}(\bar{\boldsymbol{C}}(\boldsymbol{\eta}, \dot{\boldsymbol{\eta}})\dot{\boldsymbol{\eta}} + \bar{\boldsymbol{D}}(\boldsymbol{\eta}, \dot{\boldsymbol{\eta}})\dot{\boldsymbol{\eta}} + \boldsymbol{g}(\boldsymbol{\eta})) \quad (22)$$

$$\boldsymbol{g}(\boldsymbol{\chi}_1, \boldsymbol{\chi}_2) = -\bar{\boldsymbol{M}}^{-1} \quad (23)$$

The problem is to formulate a robust controller for system (21) such that convergence in practical finite-time of tracking errors to a bounded region is achieved, even under the influence of disturbances.

Tracking errors are then defined as $\boldsymbol{e} = \boldsymbol{\chi}_{1,d} - \boldsymbol{\chi}_1$ and $\dot{\boldsymbol{e}} = \boldsymbol{\chi}_{2,d} - \boldsymbol{\chi}_2$, where $\boldsymbol{\chi}_{1,d}$ and $\boldsymbol{\chi}_{2,d}$ are the desired references. Next, the non-singular terminal mode sliding surface (Yu et al., 2005) vector is described as:

$$\boldsymbol{s} = \boldsymbol{e} + \boldsymbol{\alpha}\boldsymbol{e}_\beta \tag{24}$$

where $\boldsymbol{\alpha} = \text{diag}(\alpha_x, \ldots, \alpha_\psi)$ and $\boldsymbol{e}_\beta = [\text{sig}(\dot{e}_x)^{\beta_x}, \ldots, \text{sig}(\dot{e}_\psi)^{\beta_\psi}]^T$ with $\text{sig}(\cdot)^a = \text{sign}(\cdot)|\cdot|^a$ and constants $\alpha_i > 0$ and $1 < \beta_i < 2$ for $i = x, y, z, \phi, \theta, \psi$. Time derivative of (24) yields the following dynamics:

$$\dot{\boldsymbol{s}} = \dot{\boldsymbol{e}} + \boldsymbol{\alpha}\dot{\boldsymbol{e}}_\beta \tag{25}$$

where $\dot{\boldsymbol{e}}_\beta = [\beta_x|\dot{e}_x|^{\beta_x - 1}\ddot{e}_x, \ldots, \beta_\psi|\dot{e}_\psi|^{\beta_\psi - 1}\ddot{e}_\psi]^T$. Hence, the controller is formulated as:

$$\boldsymbol{u} = \boldsymbol{g}(\boldsymbol{\chi}_1, \boldsymbol{\chi}_2)^{-1}(\dot{\boldsymbol{\chi}}_{2,d} - \boldsymbol{f}(\boldsymbol{\chi}_1, \boldsymbol{\chi}_2) + \boldsymbol{\delta} - \boldsymbol{u}_a) \tag{26}$$

$$\boldsymbol{u}_a = -\boldsymbol{K}_1\boldsymbol{\rho} - \boldsymbol{K}_2\boldsymbol{s} \tag{27}$$

where $\boldsymbol{u}_a$ is the auxiliary control vector, $\boldsymbol{\delta} = [\frac{1}{\alpha_x\beta_x}\text{sig}(\dot{e}_x)^{2-\beta_x}, \ldots, \frac{1}{\alpha_\psi\beta_\psi}\text{sig}(\dot{e}_\psi)^{2-\beta_\psi}]^T$, $\boldsymbol{\rho} = [\text{sig}(s_x)^{\frac{1}{2}}, \ldots, \text{sig}(s_\psi)^{\frac{1}{2}}]^T$, $\boldsymbol{K}_1 = \text{diag}(K_{1,x}, \ldots, K_{1,\psi})$, and $\boldsymbol{K}_2 = \text{diag}(K_{2,x}, \ldots, K_{2,\psi})$.

The $\boldsymbol{K}_2$ matrix elements are constants such that $K_{2,i} > 0$, and matrix $\boldsymbol{K}_1$ is updated with the following adaptation law (Gonzalez-Garcia and Castañeda, 2021):

$$\dot{K}_{1,i} = \begin{cases} k_{\alpha,i}\text{sign}(|s_i| - \mu_i), & \text{if } K_{1,i} > K_{min,i} \\ K_{min,i}, & \text{if } K_{1,i} \leq K_{min,i} \end{cases} \tag{28}$$

where $\mu_i > 0$ is a fixed threshold used to identify the loss of the sliding surface. If $s_i < \mu_i$, then $K_{1,i}$ decreases at constant rate $k_{\alpha,i} > 0$ until $K_{1,i} \leq K_{min,i}$, and $K_{min,i} > 0$ is a constant defined to ensure a positive gain. Adaptive properties of $K_{1,i}$ avoid unnecessary control efforts.

4. SIMULATION RESULTS

To assess the proposed control scheme performance of Section 3, subject to disturbances, simulation results are addressed in the present section. The simulation is performed in Matlab/Simulink using a fixed-step integration time of 0.01 s with the Euler solver.

4.1 Trajectory tracking

For trajectory tracking, the VTec U-IV is dictated to track a three-dimensional helical trajectory in time $0 \leq t \leq 100$ seconds defined as:

$$\boldsymbol{\chi}_{1,d} = \begin{bmatrix} x_d \\ y_d \\ z_d \\ \phi_d \\ \theta_d \\ \psi_d \end{bmatrix} = \begin{bmatrix} 2\sin(t/4) + 0.5 \\ 2\cos(t/4) \\ 2\sin(t/80) + 0.5 \\ 0 \\ 0 \\ 0 \end{bmatrix} \tag{29}$$

The initial vehicle states are $\eta(0) = \nu(0) = [0, 0, 0, 0, 0, 0]^T$. Constant parameters used for the sliding surface vector (24) are $\alpha_x = \alpha_y = \alpha_z = 1.8$, $\alpha_\phi = \alpha_\theta = \alpha_\psi = 1$, $\beta_x = \beta_y = \beta_z = \beta_\phi = 1.5$, $\beta_\theta = \beta_\psi = 1.4$. The constant gains of the auxiliary control law (27) are defined as $K_{2,x} = K_{2,y} = 0.8$, $K_{2,z} = 0.3$, $K_{2,\phi} = K_{2,\theta} = K_{2,\psi} = 1$, and the parameter values of the adaptation law (28) are $k_{\alpha,x} = k_{\alpha,y} = k_{\alpha,z} = 0.1$, $k_{\alpha,\phi} = 2.2$, $k_{\alpha,\theta} = 0.3$, $k_{\alpha,\psi} = 1.7$, $\mu_x = \mu_y = \mu_z = \mu_\phi = \mu_\theta = \mu_\psi = 0.001$, and $K_{min,x} = K_{min,y} = K_{min,z} = 0.01$, $K_{min,\phi} = 6$, $K_{min,\theta} = 1.2$, $K_{min,\psi} = 7$, with an initial $K_{min,x}(0) = 1.4$. The parameters for the water current model are set as $\mu = 0.05$, $\kappa = 0.5$, with fixed current angles $\alpha_c = 0.2617$ rads and $\beta_c = 0.6108$ rads, and a standard deviation of $\sigma = 1$ at a frequency $f = 100$ Hz.

4.2 Discussion

The UUV trajectory shown in Fig. 2 is exhibited to be robust and reliable at tracking the desired helical trajectory. Fig. 3 show the complex disturbances induced by the water currents; the generated forces are strong, going up to 80 N. By analyzing system states in Fig. 4, the robustness of the controller against the water currents can be perceived; an initial overshoot is present in the x, z and angular states, which could be expected, as the sliding variables are in the reaching phase (Fig. 5), and there exist coupled dynamics in roll and yaw, and in surge and heave motions due to the VTec U-IV thruster configuration. Nevertheless, after 13 secs, the system reaches the surface and stabilizes, accurately tracking the varying references. At 44 secs the disturbances start rising, affecting mainly pitch and yaw, but the tracking error remains bounded at 0.1 rads. The adaptive gains shown in Fig. 6 react strongly when the disturbances are large; it can be observed that adaptive gains for the roll and yaw motions remain more active than the rest. Finally, the generated control signals for the thrusters are displayed in Fig. 7 where chattering can be perceived to be attenuated effectively. Additionally, saturation is present briefly for the majority of thruster signals, although they remain very active due to the complex disturbances.

It is worth to be noted that the range of operation of the vehicle is restricted in pitch for values [44 deg, −44 deg] due the UUV thruster configuration design, and that a singularity is present for pitch values of $\pm\frac{\pi}{2}$ rads, inherent to Euler angles.

The result reflects approximated trajectories to real-world performance as a full 6-DOF model is employed, the estimated model parameters are expected to differ few from reality, dynamic coupling is present in the motion equations, and the generated control signals are limited to the real thrusters operating range.

5. CONCLUSIONS

An adaptive non-singular terminal sliding mode controller was conceived to resolve the trajectory tracking problem of an unmanned underwater vehicle subject to induced water current forces and torques. The non-singular terminal sliding manifold ensured tracking error convergence to a region close to zero in practical finite-time. Whereas the adaptation law reduced chattering since the control gains were not overestimated and also maintained robustness. Finally, simulations were conducted in a full mathematical model, demonstrating the tracking capabilities of the proposed controller for an helical reference trajectory against disturbances.

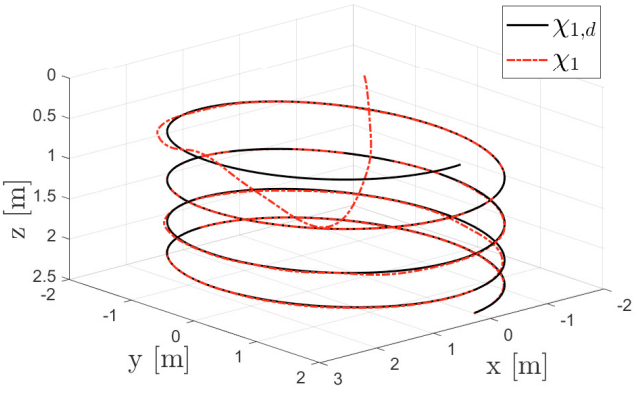

Fig. 2. Desired vs UUV trajectory

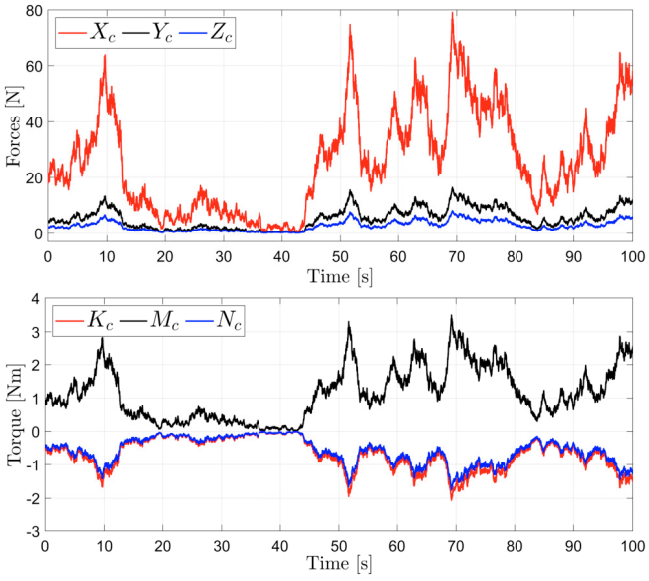

Fig. 3. Water currents induced to (top) x, y, z and (bottom) ϕ, θ, ψ

6. ACKNOWLEDGEMENTS

The authors acknowledge the support from the VantTec student group and their sponsors: Techmake Electronics, SBG Systems, NVIDIA, IFM Efector, Velodyne LiDAR, RoboNation, Google, Akky, Güntner, and Siemens. The work was also fostered by the Tecnologico de Monterrey, and the Robotics Laboratory.

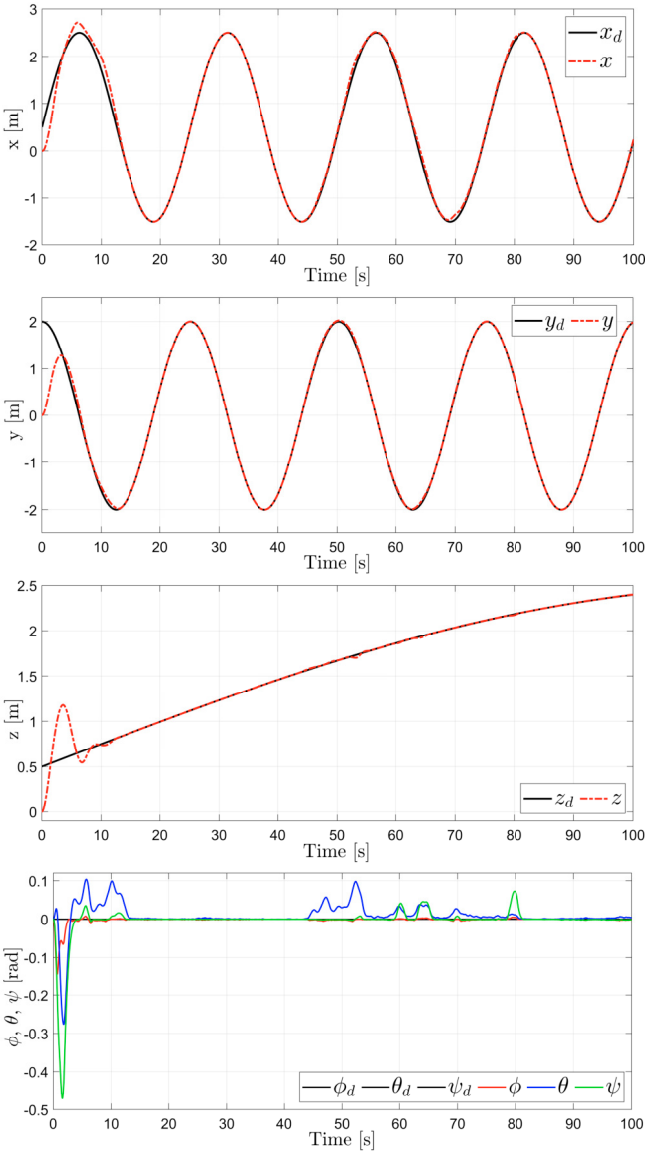

Fig. 4. UUV state responses vs desired trajectory

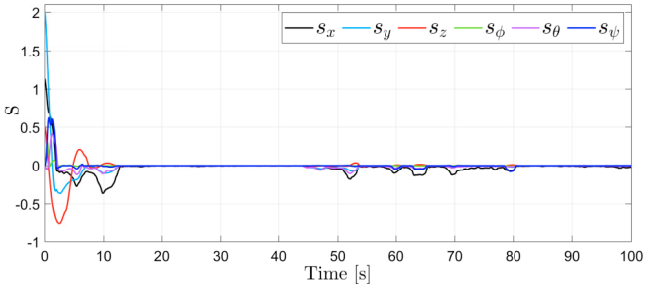

Fig. 5. Sliding surfaces

REFERENCES

Christ, R.D. and Wernli, R.L. (2014). The rov manual: A user guide for remotely operated vehicles. Butterworth-Heinemann, second edition.

Eidsvik, O. (2015). *Identification of Hydrodynamic parameters for ROVs*. Master's thesis, Norwegian Institute of Science and Technology.

Feng, Y., Yu, X., and Man, Z. (2002). Non-singular terminal sliding mode control of rigid manipulators. *Automatica*, 38(12), 2159–2167.

Fossen, T.I. (2011). *Handbook of Marine Craft Hydrodynamics and Motion Control*. John Wiley & Sons, Ltd.

Gong, P., Yan, Z., Zhang, W., and Tang, J. (2021). Lyapunov-based model predictive control trajectory tracking for an autonomous underwater vehicle with external disturbances. *Ocean Engineering*, 232, 109010.

Gonzalez-Garcia, A. and Castañeda, H. (2021). Guidance and control based on adaptive sliding mode strategy for a usv subject to uncertainties. *IEEE Journal of Oceanic Engineering*, 46(4), 1144–1154.

Hasan, M.W. and Abbas, N.H. (2022). Disturbance rejection for underwater robotic vehicle based on adaptive fuzzy with nonlinear pid controller. *ISA Transactions*.

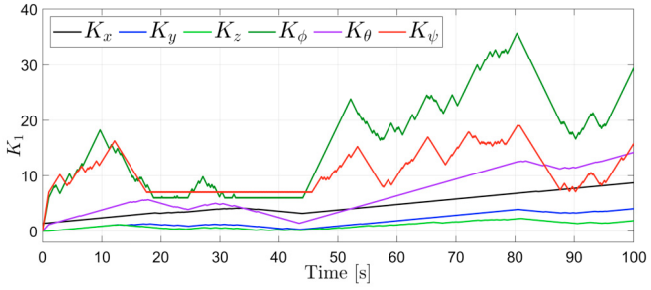

Fig. 6. Adaptive gains

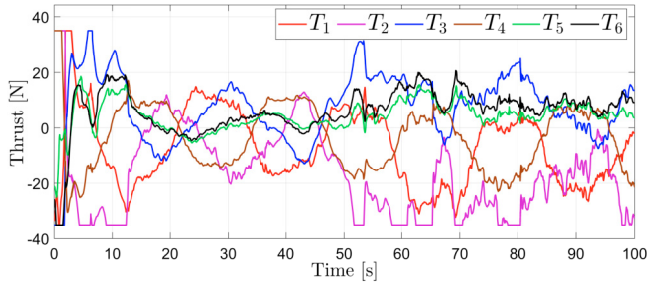

Fig. 7. Control signals

Jia, Z., Qiao, L., and Zhang, W. (2020). Adaptive tracking control of unmanned underwater vehicles with compensation for external perturbations and uncertainties using port-hamiltonian theory. *Ocean Engineering*, 209, 107402.

Karimi, H.R. and Lu, Y. (2021). Guidance and control methodologies for marine vehicles: A survey. *Control Engineering Practice*, 111, 104785.

Londhe, P.S., Dhadekar, D.D., Patre, B.M., and Waghmare, L.M. (2017). Non-singular terminal sliding mode control for robust trajectory tracking control of an autonomous underwater vehicle. In *2017 Indian Control Conference (ICC)*, 443–449.

Manzanilla, A., Ibarra, E., Salazar, S., Ángel E. Zamora, Lozano, R., and Muñoz, F. (2021). Super-twisting integral sliding mode control for trajectory tracking of an unmanned underwater vehicle. *Ocean Engineering*, 234, 109164.

Qiao, L. and Zhang, W. (2017). Adaptive non-singular integral terminal sliding mode tracking control for autonomous underwater vehicles. *IET Control Theory & Applications*, 11(8), 1293–1306.

Qiao, L. and Zhang, W. (2020). Trajectory tracking control of auvs via adaptive fast nonsingular integral terminal sliding mode control. *IEEE Transactions on Industrial Informatics*, 16(2), 1248–1258.

Rangel, M., Manzanilla, A.M., Suarez, A., Muñoz, F., Salazar, S., and Lozano, R. (2020). Adaptive non-singular terminal sliding mode control for an unmanned underwater vehicle: Real-time experiments. *International Journal of Control, Automation and Systems*, 18(3), 615–628.

Rodriguez, J., Castañeda, H., and Gordillo, J. (2020). Lagrange modeling and navigation based on quaternion for controlling a micro auv under perturbations. *Robotics and Autonomous Systems*, 124, 103408.

Shtessel, Y., Edwards, C., Fridman, L., and Levant, A. (2014). *Sliding Mode Control and Observation*. Birkhäuser Basel.

Suarez, A.E.Z., Magallanes, A.M., Rangel, M.A.G., Leal, R.L., Cruz, S.S., and Palacios, F.M. (2018). Depth control of an underwater vehicle using robust pd controller: real-time experiments. In *2018 IEEE/OES Autonomous Underwater Vehicle Workshop (AUV)*, 1–6.

Utkin, V. and Lee, H. (2006). Chattering problem in sliding mode control systems. In *International Workshop on Variable Structure Systems, 2006. VSS'06.*, 346–350.

Utkin, V.I. and Poznyak, A.S. (2013). Adaptive sliding mode control. In B. Bandyopadhyay, S. Janardhanan, and S.K. Spurgeon (eds.), *Advances in Sliding Mode Control*, chapter 2, 21–52. Springer.

Utkin, V. (1993). Sliding mode control design principles and applications to electric drives. *IEEE Transactions on Industrial Electronics*, 40(1), 23–36.

Venkataraman, S.T. and Gulati, S. (1992). Control of nonlinear systems using terminal sliding modes. In *1992 American Control Conference*, 891–893.

Wu, Y., Yu, X., and Man, Z. (1998). Terminal sliding mode control design for uncertain dynamic systems. *Systems & Control Letters*, 34(5), 281–287.

Xu, J., Wang, M., and Qiao, L. (2015). Dynamical sliding mode control for the trajectory tracking of underactuated unmanned underwater vehicles. *Ocean Engineering*, 105, 54–63.

Yu, H., Guo, C., and Yan, Z. (2019). Globally finite-time stable three-dimensional trajectory-tracking control of underactuated uuvs. *Ocean Engineering*, 189, 106329.

Yu, S., Yu, X., Shirinzadeh, B., and Man, Z. (2005). Continuous finite-time control for robotic manipulators with terminal sliding mode. *Automatica*, 41(11), 1957–1964.

Yu, X., Feng, Y., and Man, Z. (2020). Terminal sliding mode control – an overview. *IEEE Open Journal of the Industrial Electronics Society*, 2, 36–52.

Zereik, E., Bibuli, M., Mišković, N., Ridao, P., and Pascoal, A. (2018). Challenges and future trends in marine robotics. *Annual Reviews in Control*, 46, 350–368.